# Understanding Differences in Upper Stratospheric Ozone Response to Changes in Chlorine and Temperature as Computed Using CCMVal Models

A. R. Douglass, R. S. Stolarski,
S. E. Strahan, L. D. Oman

## Abstract

Projections of future ozone levels are made using models that couple a general circulation model with a representation of atmospheric photochemical processes, allowing interactions among photochemical processes, radiation, and dynamics. Such models are known as chemistry and climate models (CCMs). Although developed from common principles and subject to the same boundary conditions, simulated ozone time series vary for projections of changes in ozone depleting substances (ODSs) and greenhouse gases. In the upper stratosphere photochemical processes control ozone level, and ozone increases as ODSs decrease and temperature decreases due to greenhouse gas increase. Simulations agree broadly but there are quantitative differences in the sensitivity of ozone to chlorine and to temperature. We obtain insight into these differences in sensitivity by examining the relationship between the upper stratosphere annual cycle of ozone and temperature as produced by a suite of models. All simulations conform to expectation in that ozone is less sensitive to temperature when chlorine levels are highest because chlorine catalyzed loss is nearly independent of temperature. Differences in sensitivity are traced to differences in simulated temperature, ozone and reactive nitrogen when chlorine levels are close to background. This work shows that differences in the importance of specific processes underlie differences in simulated sensitivity of ozone to composition change. This suggests a) the multi-model mean is not a best estimate of the sensitivity of upper ozone to changes in ODSs and temperature; b) the spread of values is not an appropriate measure of uncertainty.

## 1. Introduction

Atmospheric models are used to interpret constituent observations and to predict the response of ozone to changes in composition, including the changes in stratospheric chlorine that have taken place due to release of man-made ozone depleting substances (ODSs). The Montreal Protocol and its amendments banned the production of many of these compounds beginning in 1996, and surface measurements of chlorofluorcarbons $CFCl_3$ and $CF_2Cl_2$ show that their atmospheric concentrations have leveled off and begun to decrease [*Daniel and Velders et al.*, 2007]. The effects of ODSs are expected to be easiest to quantify in the upper stratosphere because photochemical processes control the ozone level. First efforts to identify the atmospheric response to the Montreal Protocol have focused on the upper stratosphere, and *Newchurch et al.* [2003] reported evidence that the upper stratospheric ozone had ceased to decline. Presently upper stratospheric ozone is expected to increase both because of the decline in ODSs and because greenhouse gases continue to increase, cooling the stratosphere and decreasing the rate of catalytic ozone destruction as noted in *Scientific Assessment of Ozone Depletion: 2010* [*WMO*, 2011; *hereafter referred to as* WMO2011]. Attribution of changes in ozone to

1

changes in ODSs requires untangling the effects of ODSs from the effects of continuing increases in greenhouse gases [*Douglass and Fioletov et al.*, 2011].

Projections of future ozone levels are now commonly made using models that couple a general circulation model with a representation of atmospheric photochemical processes, allowing interactions among photochemical processes, radiation, and dynamics. Such models are known as chemistry and climate models (CCMs), and Stratospheric Processes and their Role in Climate (SPARC) sponsored an initiative to evaluate them (CCMVal). Metrics related to model representation of processes identified in observations were agreed upon in a series of workshops. The *SPARC CCMVal Report on the Evaluation of Chemistry-Climate Models* [SPARC CCMVal, 2010] describes in detail successes and deficiencies of participating models. These models contributed simulations to WMO2011. *Oman et al.* [2010] analyzed the various projections using multiple linear regression (MLR) and reported broad agreement among models in that. Simulated ozone principally responds to two forcings: a) prescribed surface mixing ratios for chlorine and bromine containing source gases that change the upper stratospheric amounts of chlorine and bromine (i.e., equivalent effective stratospheric chlorine (EESC)); b) prescribed boundary conditions for greenhouse gases that result in stratospheric cooling. In spite of broad agreement, ozone sensitivity to chlorine change varies among models. It is not surprising that model responses vary in the middle and lower stratosphere, where photochemical time scales become long and both photochemical and transport changes contribute to ozone change. However, even in the upper stratosphere where photochemical changes dominate, the computed ozone percentage changes, the year of return to 1980 values, and the sensitivity of ozone to perturbations in chlorine and temperature obtained vary among models.

Inspired by the CCMVal exercises, increased attention is being given to application of performance metrics and best use of the wealth of observational information obtained from satellites, including instruments on the Upper Atmosphere Research Satellite (UARS), Envisat, SciSat, and Aura, in order to arrive at the best projection for 21st century ozone. *Waugh and Eyring* [2008] assigned weights to projections of 21st century ozone based on a set of metrics that quantify model representation of processes thought to be key to ozone evolution. The weighted mean was nearly the same as the unweighted mean of all of the models that participated in the exercise, in spite of obvious differences among models and deficiencies in some models in the representation of several important stratospheric processes. *Strahan et al.* [2011] focused on the transport evaluation, with four of the models showing superior performance for both stratospheric transport and chemistry. The projections for total column ozone from these four models are more similar to each other than the ensemble of projections, and more similar than random selection of four simulations from the group of projections. The *Strahan et al.* [2011] analysis identifies the models with credible transport but did not demonstrate a direct relationship between transport deficiencies and the rate of recovery for stratospheric ozone. In several models, problems with partitioning among chlorine species, missing chemical reactions important to chlorine chemistry, or lack of conservation for the total amount of chlorine released from source gases whose mixing ratios are specified at the lower boundary impact simulated ozone recovery.

2

Similar physical concepts underlie the CCMVal models, therefore understanding why projections differ is a step towards higher confidence in predictions. This paper focuses on the upper stratosphere, where the photochemical lifetimes of ozone, fluorocarbons, and other gases like $N_2O$ are short, and transport is of little importance. This paper relies on the well-developed conceptual model for the photochemical processes that control ozone as described below, focusing on the relationship between upper stratospheric ozone and temperature as quantified for each CCMVal model to explain the variations among predictions. Our intent is to show how this relationship and its behavior in the past and present atmosphere provide insight into the differences in predicted upper stratospheric ozone levels in the 21st century [*Bekki and Bodeker et al.*, 2011].

We present the conceptual model for upper stratospheric ozone in the following section. Section 3 describes the CCMVal models and the simulations that are analyzed using this conceptual model. Results are given in section 4, with discussion and conclusions in section 5.

## 2. Conceptual model for upper stratospheric ozone

In the upper stratosphere, the time scales for formation of ozone from atomic oxygen and oxygen molecules ($O + O_2 \xrightarrow{M} O_3$, where M is a third body) and photolysis of ozone ($O_3 + hv \rightarrow O_2 + O$) are short compared to the time scales for reactions such as $O + O_3 \rightarrow 2O_2$ and catalytic cycles involving nitrogen, hydrogen and chlorine radicals that have this net effect. Bromine radicals play a minor role in the upper stratosphere and are neglected. It is convenient to define odd oxygen as the sum of ozone and atomic oxygen, using fast photochemical reactions to define their ratio ($O/O_3 \cong J_{O3}/(K_{O,O2,M}O_2M)$), and consider the production and loss to be the reactions that control their sum. Odd oxygen is produced by photolysis of molecular oxygen and destroyed by recombination reactions mentioned above. For the upper stratosphere near 2 hPa ozone is nearly equal to odd oxygen.

In the upper stratosphere transport terms can be neglected compared with the photochemical terms, and the continuity equation for odd oxygen can be written

$$\frac{\partial \gamma_{OX}}{\partial t} = P - L \qquad (1)$$

where $\gamma_{OX}$ is the odd oxygen mixing ratio, $t$ is the time, $P$ is production and $L$ is odd oxygen loss. Chapter 6 of the CCMVal report includes a comparison of the photolysis rates as determined by several chemistry-climate models. The values for the photolysis rate of molecular oxygen ($J_{O2}$) are not constant across the CCMVal models; differences in production are likely responsible for some part of the differences in the ozone mixing ratio. As will be shown below, the ozone sensitivity to temperature also varies with ozone level. However, differences in photolysis will be insensitive to changes in composition, and it is possible to understand much of the variation in the diagnosed

response of model-computed ozone to changes in chlorine and temperature by focusing on the loss terms as will be shown in section 4. Assuming small perturbations in $\gamma_{OX}$ and temperature ($T$), assuming balance between production and loss ($P \cong L$), and neglecting perturbations to the production term, the continuity equation becomes

$$\frac{\partial \gamma'_{OX}}{\partial t} = -\frac{\partial L}{\partial \gamma_{OX}} \gamma'_{OX} - \frac{\partial L}{\partial T} T' \qquad (2)$$

or

$$\frac{\partial \gamma'_{OX}}{\partial t} = -\Gamma \gamma'_{OX} - \Theta T' \qquad (3)$$

where $\Theta \equiv \partial L / \partial T$ and $\Gamma \equiv \partial L / \partial \gamma_{OX}$, following the notation of *Stolarski and Douglass* [1985] (hereafter referred to as SD1985). Equation 3 reduces to $\gamma'_{OX} = -\frac{\Theta}{\Gamma} T'$ when the perturbation does not very with time. The inverse relationship between ozone and temperature is found because loss processes for ozone are more efficient at warmer temperatures. In early observational studies such a relationship between ozone and temperature was broadly interpreted to indicate dominance of photochemical processes over transport processes [*Wang et al.,* 1983; *Nagatani and Miller,* 1984]. *Rood and Douglass* [1985] showed that spatial perturbations in temperature produced by wave motions could lead to an inverse correlation between ozone and temperature through photochemical processes, but, depending on the horizontal gradients in odd oxygen, these wave motions could also necessitate accounting for transport terms. Here we focus on the relationship between $\gamma' = \gamma - \bar{\gamma}$ and $T' = T - \bar{T}$ where the overbar indicates annual zonal average and $\gamma'$ and $T'$ are deviations of the zonal means from their annual average values. We focus on 2 hPa for two reasons: chlorine catalyzed loss (and therefore chlorine change) is important to the ozone level and photochemical time scales are short enough that transport can be neglected when considering perturbations from the annual zonal mean.

Apart from providing information about the relative importance of photochemistry and transport processes, the relationship between ozone and temperature provides information about the mix of cycles contributing to ozone loss. *Barnett et al.* [1975] pointed out that the temperature dependence of equilibrium ozone concentration as derived from observations could be compared with that expected based on the mix of loss processes associated with different photochemical theories. SD1985 built on the use of rate limiting steps for the catalytic cycles important to ozone destruction as discussed by *Johnston and Podolske* [1978] to develop a parameterization with explicit representation of catalytic loss processes. For convenience, the rate limiting reactions for odd oxygen loss are given in Table 1. The SD1985 approach emphasizes that the catalytic loss cycles associated with hydrogen, chlorine and nitrogen species make different contributions to the overall sensitivity of ozone to temperature. Recombination of $O + O_3$ and catalytic

4

cycles with the same effect all contribute to $\Gamma$, the loss frequency (inverse of the photochemical lifetime).  Following SD1985

$$Loss = Loss_{OX} + Loss_{NOX} + Loss_{HOX} + Loss_{ClX} \qquad (3)$$

$$\Gamma = \Gamma_{OX} + \Gamma_{NOX} + \Gamma_{CLX} + \Gamma_{HOX} \qquad (4)$$

$$\Theta = \Theta_{OX} + \Theta_{NOX} + \Theta_{ClX} + \Theta_{HOX} \qquad (5)$$

The ratio $\Theta/\Gamma$ that quantifies the linear relationship between $\gamma'_{OX}$ and $T'$ depends on the balance of loss processes.  The reaction $O + O_3$ is the most temperature dependent; the catalytic cycle involving chlorine is the least.  A model with higher ozone levels for any reason (greater production, less loss, cooler temperature) will be more sensitive to a temperature perturbation than a model with lower ozone because $O + O_3 \rightarrow 2O_2$ will be more important in (3) and its contribution to $\partial L/\partial T$ is proportional to $\gamma^2_{OX}$ [SD1985].

A similar argument can be applied to the sensitivity of ozone to chlorine change.  The ozone response to a composition change will depend mainly on the change in the balance of loss processes relative to the balance of processes in the base state. Note that for the upper stratosphere production is nearly equal to loss, so the net loss is similar in both the perturbed and base states.  An increase in the chlorine contribution to loss causes ozone to decrease (along with other changes in the partitioning of short lived species) such that the net loss is nearly unchanged.  The contributions of other loss processes to the balance also affect ozone sensitivity to chlorine change. For example, for models that produce the same upper stratospheric temperature, a simulation in which the nitrogen loss cycle is more important will be less sensitive to chlorine change than a simulation in which the nitrogen loss cycle is less important.  We do not consider changes in photolysis of molecular oxygen due to change in overhead column ozone because such effects are minimal for small changes in composition.

These concepts have been applied broadly.  Observational and theoretical studies discuss the dependence of the modeled response on the simulated mix of loss processes [e.g., *Douglass et al.*, 1985; *Douglass et al.*, 1986; *Froidevaux et al.*, 1989; *Smith*, 1995].  Such a linear relationship has been used in simulations to study the response of ozone to temperature variations due to planetary waves [e.g., *Hartmann and Garcia*, 1979; *Randel*, 1993; *McCormack et al.*, 2006].  *Hood and Douglass* [1988] applied the same formalism to the ozone and temperature responses to short term variation in solar ultraviolet radiation. *Chandra et al.* [1993] compared the annual variation of ozone as observed by Solar Backscatter Ultraviolet radiometers with that simulated using a two-dimensional model with specified temperatures, noting that the observations and model were in better agreement if the chlorine catalyzed ozone loss was less important.  At that time this work supported the conjecture that products of the reaction $ClO + OH$ included $HCl + O_2$ in addition to $Cl + HO_2$.  The $HCl$ product channel reduces $ClO$ relative to total inorganic chlorine ($Cl_Y$) in the upper stratosphere, thereby reducing the importance of chlorine-catalyzed loss and increasing the sensitivity of ozone to the annual cycle in temperature.

Laboratory experiments provide the branching ratio for this experiment that is used in current models [*Lipson et al.,*1999; *Sander et al.,* 2011].

The relationship between ozone and temperature can also be used to show how the mix of loss processes changes due to composition change. *Douglass and Rood* [1986] used 1979 data from the Limb Infrared Monitor of the Stratosphere (LIMS) to derive photochemical information from the spatial perturbations in ozone and temperature, suggesting that the ozone sensitivity to temperature would decrease as chlorine increased in importance. *Stolarski et al.* [2011] argue that observed changes in the sensitivity of ozone to temperature as chlorine decreases are useful in attribution studies to separate effects of chlorine decrease from the effects of greenhouse gas increase on ozone.

It is conceptually straightforward but algebraically complex to compute the dependence of $\Gamma$ and $\Theta$ on changes in ozone, temperature and chlorine ($\gamma_{OX}$, T and $\gamma_{Cl}$) by differentiating the expressions for $\Gamma$ and $\Theta$ found in SD1985. Here $\Gamma$ is a function of $\gamma_{OX}$, $\gamma_{Cl}$, and T. A result of weak sensitivity of chlorine catalyzed loss to temperature is that the contribution of $\Theta_{ClX}$ to $\Theta$ is small compared to contributions from other loss terms Because we are focused on the upper stratosphere near 2 hPa where the effects of chlorine change are the largest, we keep only the leading terms that contribute to $\Gamma$ and $\Theta$, ignoring terms that couple loss cycles through interference reactions that are important in the middle and lower stratosphere. After differentiating and rearranging, we obtain the following expressions for the logarithmic derivative of $\Theta$ due to changes in temperature and odd oxygen mixing ratio:

$$\frac{\Delta\Theta}{\Theta} = \left\{ \frac{\Theta_{OX}}{\Theta}\left(\frac{2060}{T} - 4120\right) + 2.4\frac{\Theta_{NOX}}{\Theta} \right\}\frac{\Delta T}{T}$$
$$\left\{ \frac{2\Theta_{OX} + \Theta_{NOX} + \Theta_{HOX}}{\Theta} \right\}\frac{\Delta\gamma_{OX}}{\gamma_{OX}} \tag{6}$$

It is straightforward to show the first term on the right, the contribution due to the fractional change in temperature, is small compared with the second term, the contribution due to the fractional change in odd oxygen mixing ratio that is primarily due to chlorine change. Noting that $\Theta \approx \Theta_{OX} + \Theta_{NOX} + \Theta_{HOX}$, equation (6) is approximated

$$\frac{\Delta\Theta}{\Theta} \cong \left(1 + \frac{\Theta_{OX}}{\Theta}\right)\frac{\Delta\gamma_{OX}}{\gamma_{OX}} \tag{7}$$

The implicit dependence of hydrogen catalytic loss cycles on the odd oxygen mixing ratio described in detail in SD1985 complicates the expression that is obtained by differentiating the expressions for $\Gamma$. However, for the limited altitude domain considered here the direct dependence on the odd oxygen mixing ratio is most important, and the expression for the logarithmic derivative of $\Gamma$ is approximated

$$\frac{\Delta\Gamma}{\Gamma} \cong \left\{\left(1 + \frac{\Gamma_{OX}}{\Gamma}\right)\frac{\Delta\gamma_{OX}}{\gamma_{OX}} + \frac{\Gamma_{CL}}{\Gamma}\frac{\Delta\gamma_{CL}}{\gamma_{CL}}\right\} \qquad (8)$$

We combine equations (7) and (8) to obtain a remarkably simple expression for the logarithmic derivative of $\Theta/\Gamma$:

$$\frac{\Delta(\Theta/\Gamma)}{\Theta/\Gamma} \cong \left[\frac{\Theta_{OX}}{\Theta} - \frac{\Gamma_{OX}}{\Gamma}\right]\frac{\Delta\gamma_{OX}}{\gamma_{OX}} - \frac{\Gamma_{Cl}}{\Gamma}\frac{\Delta\gamma_{Cl}}{\gamma} \qquad (9)$$

The first term on the right depends on the contribution of $O + O_3 \rightarrow 2O_2$ to the net ozone loss compared with other cycles. The contributions of $\Theta_{OX}$ to temperature sensitivity and $\Gamma_{OX}$ to loss frequency (inverse lifetime) are greater when this process is more important to net loss and vice versa. At 2 hPa the quantity in brackets is always positive and less than 1 since $O + O_3$ is more important to the temperature sensitivity than to inverse lifetime. The absolute contribution of the second term is the same sign as the first term, since $\frac{\Delta\gamma_{OX}}{\gamma_{OX}}$ is opposite sign of $\frac{\Delta\gamma_{Cl}}{\gamma_{Cl}}$. The ozone sensitivity to temperature deviations $(S \equiv -\Theta/\Gamma)$ is therefore expected to vary with chlorine change. Furthermore, the ozone sensitivity to temperature for a given model depends on the relative importance of odd oxygen loss to the other loss processes (first term in (9)) and on the importance of chlorine loss to the total loss (second term in (9)) and thus values obtained for $S$ likely vary among models. Note that (9) was derived for small perturbations, and the perturbation to chlorine from the early 1960s to the late 1990s is not small. We evaluate these terms by selecting periods with changes in inorganic chlorine less than 25%.

## 3. Models and Data
### 3.1 CCMVal Models

*Morgenstern et al.* [2010] present a detailed overview of the models that participated in the second round of the CCMVal activity. These models contributed simulations that are evaluated in the CCMVal report [SPARC] and that are used in two chapters of WMO2011: a) Chapter 2 (Stratospheric Ozone and Surface Ultraviolet Radiation [*Douglass and Fiolevtov et al.*, 2011]); b) Chapter 3 (Future Ozone and Its Impact on Surface UV [*Bekki and Bodeker et al.*, 2011]. Eighteen groups contributed simulations to this activity, but for this analysis we include only fourteen models with a vertical domain that includes the upper stratosphere and contributed a future simulation. The future simulation (referred to as REF-B2) uses the A1B greenhouse gas scenario from the Intergovernmental Panel on Climate Change (IPCC) [2000] and the revised A1 halogen scenario from WMO [2007] and SPARC CCMVal [2010]. Most models have simulations that cover 1960 – 2099. The Unified Model/United Kingdom Chemistry Aerosol Community Model – Met Office (UMUKCA-METO) is an exception in that their future simulation ends in 2083. *Oman et al.* [2010] provide details about the

scenarios and the other inputs to these simulations.

## 3.2 *Data*

The primary intent of this paper is to demonstrate that the differences in simulations can be interpreted and understood. We make no attempt to identify 'best' simulations that agree with one or more sets of observations. However, it is useful to include some observations that show that the seasonal cycles in upper stratosphere ozone and temperature and establish a context for discussion. Data shown here are from two sources, the Microwave Limb Sounder (MLS) on the Aura satellite [*Waters et al.,* 2006], and from the Halogen Occultation Experiment (HALOE) on the Upper Atmosphere Research Satellite (UARS) [*Russell et al.,* 1993].

MLS began measurements in August 2004 and continues to measure profiles of a suite of constituents of stratospheric importance. Here we consider only ozone and temperature. According to the data quality document [*Livesey et al.,* 2011], MLS V3.3 ozone accuracy at 2 hPa is 5%. The accuracy of the temperature profiles is estimated to be a few degrees. For our comparisons we use the MLS annual mean ± 2K. As will be shown below the range of simulated values for the annual mean during the MLS era is about 25K, much larger than any realistic estimate of accuracy derived from comparisons with other temperature estimates.

HALOE measured profiles of a suite of constituents of stratospheric importance from late 1991 until late 2005 using solar occultation. We use HALOE profiles of $NO$ and $NO_2$ to estimate the total reactive nitrogen ($NO_Y$) at 2 hPa. *Gordley et al.* [1996] discuss validation of these constituents. Because $NO_Y$ varies temporally and because HALOE sampling is not uniform, we obtain an estimate for annually averaged $NO_Y$ from HALOE but consider any simulation result within a 1-2 parts per billion of the HALOE estimate to be equally possible.

## 4. Results

In the midlatitude upper stratosphere, the annual means of zonal mean ozone and temperature vary markedly among the CCMVal models. These mean values exhibit similar temporal behavior to each other for 1960 – 2100, but significant biases among the models persist throughout the integration. Time series of annual mean ozone and temperature that are typical for the upper stratosphere are shown in Figure 1 for 50°N, 2 hPa. In 1960, stratospheric chlorine was close to its natural level, and simulated ozone varies among models both due to differences in the photolysis of molecular oxygen that controls odd oxygen production and due to differences in loss (i.e., differences in levels of reactive odd nitrogen and hydrogen that affect catalytic loss cycles directly and also differences in temperature that affect loss through the temperature dependence of photochemical reactions).

Chapter 3 of *SPARC CCMVal* [2010] discusses temperature biases and their possible relationship to biases in ozone and water vapor, concluding that deficiencies in the radiation codes are the main driver of temperature differences. For the CCMs used here,

higher ozone levels are associated with lower temperatures, consistent with the conclusion that the temperature biases indicate differences in the radiative part of the CCMs. The range of temperature and ozone values obtained from the CCMVal models for identical boundary conditions provides an opportunity to test the conceptual model described in section 2. Figure 1 shows that the CCM with the lowest temperatures in the upper stratosphere produces the highest ozone values and that the CCMs with the warmest temperatures tend to produce lower ozone values. We test the conceptual model by calculating the differences of each model from the 1960 multi-model mean, $\Delta T = T_i - \overline{T}^{MM}$ and $\Delta \gamma = \gamma_i - \overline{\gamma}^{MM}$ where the subscript $i$ represents a single model, and overbar with superscript MM indicates the multi-model mean. These differences are anti-correlated, with $r^2$ of -0.75, suggesting that the temperature differences are responsible for a significant part of the spread in the simulated ozone values. To test if this interpretation quantitatively follows the conceptual model, we use multiple linear regression following *Oman et al.* [2010] to obtain values for $S$ (the sensitivity of ozone in each CCMVal model to a temperature perturbation $S_i = \partial \gamma_i / \partial T_i$, where the subscript $i$ again refers to a single model), and use these coefficients to estimate how much of the difference from the multi-model mean is explained by the simulated sensitivity to temperature and the temperature difference relative to the multi-model mean. The ozone differences from the multi-model mean expected from the temperature differences ( $S_i \Delta T$ ) are compared with the ozone differences from the multi-model mean ( $\Delta \gamma_{OX}$ ) in Figure 2. This comparison shows that much of the variation in ozone among models is a result of the differences in temperature. The results in Figure 2 are quantitatively similar whether using values for $S_i = \partial \gamma_{OX} / \partial T$ obtained for each model from multiple linear regression or using values obtained from the ozone and temperature annual cycles.

The 1960 spread in ozone values among the models is greater than 2 ppmv; the multi-model mean and standard deviation are 5.51 and 0.55 ppmv respectively. The individual model sensitivity to temperature times the difference in each model temperature from the multi-model mean accounts for about half of the spread in 1960 ozone values. The standard deviation in ozone values after accounting for the temperature difference is reduced to 0.34 ppmv. The largest differences from multi-model mean ozone are nearly equal to those expected from the temperature difference and derived sensitivity of ozone to temperature. Differences in the mix of loss processes also contribute to the spread in ozone values shown in Figure 1. This is illustrated but not quantified by coloring the points in Figure 2(a) according to the local mixing ratio for total reactive nitrogen ($NO_Y$). The points with low values of $NO_Y$ tend to appear on the high side of the 1:1 line, thus larger ozone anomalies are consistent with colder temperatures, and less loss due to the nitrogen loss cycle. The converse is also true. The mixing ratio for water also varies among models, contributing to different levels of hydrogen radicals, but the hydrogen loss cycles are less important than the nitrogen loss cycle at this altitude (SD1985).

It is useful here to notice how well the various models reproduce observed values for ozone, temperature, and $NO_Y$. Figure 2(b) is a scatter plot for 2006 simulated temperature vs. ozone mixing ratios 50°N 2 hPa. The cross indicates values for these quantities computed from measurements obtained within 2 degrees latitude by the Aura MLS. Several thousand profiles contribute to the mean, thus the standard error of the mean is

miniscule. The height and width of the cross reflect the estimates of accuracy as discussed above. Figure 2(b) also supports the statements above that the simulated ozone levels are higher for cooler temperatures and vice versa. Even in 2006, when the upper stratospheric ozone is less sensitive to temperature due to the importance of the chlorine catalyzed loss cycle, the models with cooler temperatures tend to have higher ozone and vice versa.

Although $NO_y$ varies temporally in all of the models, the effect of the temporal increase in the boundary condition for $N_2O$ (the source of nitrogen radicals) is opposed by the effect of cooling temperatures [*Rosenfield and Douglass*, 1998], and the differences among models in upper stratospheric $NO_Y$ are much larger than the trend. Since $NO_Y \sim NO + NO_2$ at this pressure, we obtain an estimate for annual mean $NO_Y$ from the multi-annual time series of observations obtained by the UARS HALOE [*Reber et al.*, 1993]. HALOE is an occultation instrument and measures 13-15 profiles per day at each of two latitudes. Middle latitude $NO_Y$ varies seasonally, and HALOE sampling is not uniform. The data indicate ~ 12 ± 1-2 ppbv for annual zonal mean for $NO_Y$ at 50°N, 2 hPa. In Figure 2(a), low $NO_Y$ may account for the somewhat larger difference from multi-model mean $O_3$ than explained by the cooler than multi-model mean temperature for the two models with the largest positive $O_3$ differences. The largest positive difference from the multi-model mean temperature is consistent with ~ -1 ppmv difference in $O_3$. The model $NO_Y$ from this model is generally consistent with HALOE. A cluster of models with very small temperature differences from the multi-model mean have $NO_Y$ values that are above, below and consistent with the HALOE estimate.

Observed annual mean values for ozone, temperature and $NO_Y$ are included as a point of reference, and generally illustrate how the computed ozone and its sensitivity to temperature conform to expectations that follow from the conceptual model described above. These comparisons also attest to the difficulty in producing simultaneous agreement with observations for all of these quantities. Figure 2(b) shows that most simulations are warmer and have lower ozone than observed by MLS. Two models have mean ozone approximately equal to the MLS mean; for one model temperature and $NO_Y$ are also comparable to observed values but the other model is cold compared with MLS and $NO_Y$ is too low compared HALOE.

Note that the shapes of the temperature time series (Figure 1(b)) are more similar to each other than the shapes of the ozone time series (Figure 1(a)). This shows that the simulated radiative response of temperature to the change in greenhouse gases is more similar among the models than the simulated photochemical response of ozone. In most of the simulations the rate of change of temperature with time decreases around 2000, when chlorine stops increasing. This change in slope, discussed by *Stolarski et al.* [2010], occurs because greenhouse gas increase and ozone loss due to anthropogenic chlorine both affect temperature. Prior to the late 1990s, anthropogenic chlorine is increasing and these processes act in the same sense. Once anthropogenic chlorine begins to decrease these processes oppose each other.

The differences among ozone profiles are much smaller in 2000 than they were in 1960 when chlorine levels in the stratosphere were not greatly elevated compared with the natural background. Chlorine catalyzed ozone loss is nearly independent of temperature [SD1985], thus the balance of ozone loss processes and the ozone level are more similar among the models when the chlorine term is most important. After 2000 the time series diverge as chlorine decreases. We compute the standard deviation of the annual zonal means from the group of models for each year to show quantitatively that the simulations are more similar when chlorine is elevated. Figure 3 shows this standard deviation at 50°N 2hPa as a function of chlorine amount from one of the models. Although there are differences among models in the chlorine amount at 2 hPa, the time dependence largely follows the boundary conditions and the conclusion drawn from this figure is the same using chlorine amount from any model. The standard deviation for maximum chlorine is reduced by nearly 50% compared to its value for 1960 chlorine. This near linear dependence of the standard deviation of ozone from the CCMVal models on chlorine amount is found throughout the upper stratosphere.

Given the differences in ozone, temperature and the mix of loss processes, it is not surprising that the sensitivity of ozone to temperature ($\partial\gamma_{O3}/\partial T$) and its sensitivity to inorganic chlorine ($\partial\gamma_{O3}/\partial\gamma_{Cl}$), both obtained through application of MLR to the ozone time series, vary among the models. The ozone sensitivity to chlorine and temperature are shown as functions of 1960 ozone in Figure 4(a) and (b) respectively. The ozone sensitivity to chlorine is nearly linearly related to the 1960 ozone level (Figure 4(a)), with one obvious outlier. In all panels of Figure 4 the sensitivity indicated by a star (*) is the MRI model that omitted $ClO + OH \rightarrow HCl + O_2$ (see Chapter 6 of *SPARC CCMVal* [2010]). This difference in chemical mechanism shifts the partitioning of inorganic chlorine towards $ClO$, increasing the sensitivity of ozone to chlorine since $ClO + O$ is the rate-limiting step for chlorine-catalyzed catalytic ozone destruction. Eliminating the MRI model just for this calculation, the correlation coefficient between 1960 ozone and sensitivity to $\gamma_{Cl}$ is 0.9; the dashed line in Figure 4(a) is the linear fit.

Figure 4(a) shows that the sensitivity of ozone to $\gamma_{Cl}$ depends on the unperturbed ozone level, implying dependence on net production and on the balance among loss processes other than chlorine. For simulations with the same chemical mechanism, it does not matter exactly what combination of photolysis of $O_2$, temperature, nitrogen species and hydrogen species leads to higher or lower ozone levels. The simulations with lower ozone in 1960 are associated with greater contributions to loss from cycles other than $O + O_3$, thus addition of chlorine makes a smaller relative increase in loss and the simulation is less sensitive to $\gamma_{Cl}$. Conversely, the simulations with higher ozone in 1960 have less loss due to cycles other than $O + O_3$, addition of chlorine is of greater relative importance, and the sensitivity to $\gamma_{Cl}$ is greater.

The ozone sensitivity to temperature also depends on the ozone amount (Figure 4(b)), although with much more scatter than the ozone sensitivity to $\gamma_{Cl}$. Simulations with higher ozone levels are more sensitive to temperature because the odd oxygen loss cycle is the most temperature dependent. The ozone sensitivity to temperature shown in Figure 4(b) also depends on the relative importance of the catalytic cycles involving nitrogen

11

and hydrogen species, because the catalytic cycle involving nitrogen species is more temperature dependent than the cycles involving hydrogen species at this altitude [SD1985].

Figure 4(c) shows the ozone sensitivity to temperature as obtained from the annual cycles as a function of 2007 ozone. As will be discussed in more detail below, in all of the simulations ozone is less sensitive to temperature in 2007 than in 1960 due to the increased importance of chlorine-catalyzed loss. A black cross indicates values of ozone and the sensitivity of ozone to temperature obtained from the annual cycle as observed by MLS; the size of the cross corresponds to 5% errors in ozone 10% errors in the sensitivity of ozone to temperature. Simulated ozone levels and sensitivity of ozone to temperature are always less than the mean values obtained from MLS, although a few models produce values within the error limits.

*Chandra et al.* [1993] discuss the variation of the seasonal cycle of ozone due to change in the mix of loss processes. Clearly as $\gamma_{Cl}$ increases and ozone decreases due to chlorine-catalyzed loss, the importance of the most temperature dependent of the loss processes $O + O_3$ decreases. At the same time, the importance of the least temperature dependent of the loss processes $ClO + O$ increases. We compute the sensitivity of ozone to temperature $S = -\Theta/\Gamma$ each year for each of the CCMVal models using a least squares fit to relate the annual cycles of ozone and temperature.

A time series for $S$ is obtained for each model; these are shown in Figure 5(a) and all conform to expectation. For each model, $S$ decreases until about 2000 as $\gamma_{Cl}$ increases, chlorine catalyzed ozone loss becomes more important and ozone deceases. After 2000 $S$ increases as $\gamma_{Cl}$ decreases towards its natural level. The values of $S$ for each model vary due to differences in ozone, temperature, and the relative importance of the catalytic cycles that contribute to ozone destruction.

Figure 5(b) shows the timeseries from 5(a) normalized by their respective 100 year means (i.e., $S/\overline{S}$, where the overbar indicates the 100 year mean). This normalization emphasizes the relative changes in the annual cycle amplitude that are due to composition change. The models' normalized timeseries are remarkably similar to each other. Even the relative behavior of $S/\overline{S}$ from MRI conforms, following the conceptual model presented in section 2, in spite of the missing reaction in the photochemical scheme that leads to higher values for the $ClO$ mixing ratio relative to $\gamma_{Cl}$ and greater importance for chlorine catalyzed loss as discussed above. The rate-limiting steps of the catalytic loss cycles, and their magnitudes relative to each other, control the time dependence of $S/\overline{S}$ without regard to why one or another loss cycle is more or less important. Note that although there are differences among models that affect both their absolute level of $\gamma_{Cl}$ and partitioning among the chlorine containing species, the overall time dependence of chlorine and the relative changes in chlorine containing species are specified by the boundary conditions. The time dependence of $S/\overline{S}$ conforms across the models because the efficiency of the chlorine catalyzed loss is proportional to the $ClO$ level and the fractional changes in $ClO$ are mainly controlled by the boundary conditions.

The temporal dependence of $S/\overline{S}$ can be used to obtain a final test of the conceptual model as described in section 2. *Stolarski et al.* [2011] show that the temporal dependence of $S/\overline{S}$ is small for a simulation that considers climate change without chlorine change. We neglect the first term on the right-hand side of (9) and rearrange to obtain the following difference equation:

$$\left(\frac{\Delta S}{S}\right)\bigg/\left(\frac{\Delta \gamma_{Cl}}{\gamma_{Cl}}\right) \approx \frac{\Gamma_{Cl}}{\Gamma} \qquad (10)$$

This equation shows that the logarithmic derivative of the sensitivity of ozone to temperature, obtained from the annual cycle, divided by the logarithmic derivative of inorganic chlorine is a measure of the importance of chlorine-catalyzed loss to relative to the total ozone loss. We evaluate the left side of equation 10 for the chlorine change from 1.75 ppbv to 2.25 ppbv as obtained from each of the CCMVal models, using parts of each timeseries where $\gamma_{Cl}$ increases and decreases. Figure 6 shows the values for the left side of equation 10 as a function of simulated $NO_y$. This result follows directly from the conceptual model and shows that the chlorine catalyzed loss produces a larger change in ozone annual cycle in simulations with lower $NO_y$ and vice versa. As discussed above, other factors contribute to the balance of loss processes, and lead to scatter.

Overall, this analysis explains the differences in response of the CCMVal models to changes in anthropogenic chlorine and greenhouse gases using the conceptual model presented in section 2. The simulated temperature in the unperturbed state is important; differences in 1960 simulated temperature account for half of the differences in 1960 ozone levels. The differences in temperature also affect the sensitivity of ozone to changes in chlorine in temperature, because simulated ozone is more sensitive to changes in $\gamma_{Cl}$ if $O + O_3$ is more important. Simulated ozone is also more sensitive to temperature change if ozone levels are higher because $O + O_3$ is the most temperature dependent loss processes. The normalized sensitivity of ozone to temperature evolves in a similar manner for all models because the boundary conditions control the temporal dependence of upper stratospheric chlorine. Finally, the relative change in ozone sensitivity to temperature divided by the relative change in chlorine (the left side of equation 10 above) varies among models. The conceptual model indicates that this ratio provides a measure of the importance of chlorine catalyzed loss relative to total loss. The relationship of this ratio to simulated $NO_Y$ shown in Figure 6 supports this interpretation.

## 5. Discussion and Conclusions

This analysis shows that much of the spread in the 1960 simulated values seen in Figure 1 as well as the spread in the predictions for annual average upper stratospheric ozone are explained using the well-developed conceptual model for ozone photochemistry. This analysis reinforces statements that have been made often over the past decades – simulated responses to perturbations in $\gamma_{Cl}$ or $T$ depend on the simulated balance of loss processes in the unperturbed atmosphere. The ozone sensitivity to changes in chlorine and temperature as computed from simulations provided by the CCMVal models depends on their computed ozone level in 1960, when chlorine loading is perturbed by only a few

tenths of a ppbv above background. This analysis shows that quantitative simulation of upper stratospheric ozone evolution requires accurate simulation of base state values for ozone, temperature and reactive nitrogen. The analysis also shows that the range of ozone values produced by the CCMVal models will converge if the range of simulated temperatures is reduced by improvements to the radiation schemes (see Chapter 3 of *SPARC CCMVal* [2010]).

Although in this paper the analysis of response to composition change focused on a single latitude and pressure surface, the results are general in that the sensitivities of ozone to chlorine and temperature change computed at this level correlate with the response at other locations and to the integrated response for the upper stratosphere. For example the correlation coefficient between the sensitivities to $\gamma_{Cl}$ at 50°N 2 hPa and the sensitivity of the partial ozone column for 20 – 0.1 hPa averaged between 60°S and 60°N computed using MLR is 0.85.

Most of the simulations do not produce values of ozone, temperature and $NO_Y$ within the uncertainty range of the observations of all three. This analysis highlights the importance of verifying that a model produces appropriate upper stratospheric temperature and balance of loss processes if attempting to use a simulation along with observations to untangle the dependence of observed ozone changes on changes in chlorine and temperature. Such an effort can only be successful if simulated values for all three fall within boundaries dictated by observations. If these conditions are met, the approach can be useful in attribution studies. For example, *Stolarski et al.* [2011] use the same conceptual model to argue that a signature of the change in importance of chlorine to ozone loss can be obtained from the sensitivity of ozone to temperature as determined by analysis of their annual cycles.

For the upper stratosphere, this analysis demonstrates the weakness of using a multi-model mean to obtain a 'best estimate' for future ozone levels. The different responses from these simulations are expected given differences in temperature, $NO_Y$ and ozone when chlorine levels are near background, and averaging over such responses blurs the understanding of the differences in sensitivity to chlorine that arise from the broad set of initial conditions (Figure 1). For the simulations shown here, the model that uses the accepted chemical mechanism and is most sensitive to chlorine is also the coldest and has unrealistically low $NO_Y$. Understanding of the upper stratospheric sensitivity to chlorine change and confidence in prediction are enhanced by analysis that reveals the cause of this difference in sensitivity to chlorine. The multi-model mean masks the differences. Furthermore, it is clear from this analysis that the range of simulated responses is related to differences in composition and climate that can be judged realistic or not using measurements. It is therefore not appropriate to interpret this sort of range in sensitivity as a measure of uncertainty.

The key result of this work is that it is possible to apply the conceptual model to interpret the differences in the CCMVal model projections for upper stratospheric ozone. The analysis of *Oman et al.* [2010] shows variations in the projected level of ozone and in the sensitivity of ozone to chlorine change and temperature change derived from MLR. This

analysis takes an additional step, building on the foundation of ozone photochemistry developed over decades and explaining the differences in the ozone sensitivity to chlorine and temperature. Identifying the processes that control the differences among simulations of present day ozone is a necessary step towards understanding the differences in ozone projections. Improved prediction and confidence therein follow.

The upper stratosphere is the focus of this initial effort because of the simplicity of the conceptual model. *Strahan et al.* [2011] show that the transport diagnostics can be used to separate predictions for total ozone. It is our intention to apply the methodology of the present work to obtain quantitative explanation of the photochemical and transport changes that lead to variance in the projections of lower stratospheric ozone and the ozone column.

# References

Akiyoshi, H., L. B. Zhou, Y. Yamashita, K. Sakamoto, M. Yoshiki, T. Nagashima, M. Takahashi, J. Kurokawa, M. Takigawa, and T. Imamura (2009), A CCM simulation of the breakup of the Antarctic polar vortex in the years 1980–2004 under the CCMVal scenarios, *J. Geophys. Res., 114*, D03103, doi:10.1029/2007JD009261.

Austin, J., and R. J. Wilson (2006), Ensemble simulations of the decline and recovery of stratospheric ozone, *J. Geophys. Res., 111*, D16314, doi:10.1029/2005JD006907

Barnett, J. J., J. T. Houghton and J. A. Pyle (1975), The temperature dependence of the ozone concentration near the stratopause, *Quart. J. R. Met. Soc. 101*, 245-257.

Bekki, S. and G. E. Bodeker (Coordinating Lead Authors) et al. (2011), Future ozone and its impact on surface UV, Chapter 3 in *Scientific Assessment of Ozone Depletion: 2010*, Global Ozone Research and Monitoring Project – Report No. 52, 516 pp., World Meteorological Organization, Geneva, Switzerland.

Chandra, S., C. H. Jackman, A. R. Douglass, E. L. Fleming and D. B. Considine (1993), Chlorine catalyzed destruction of ozone – implications for ozone variability in the upper stratosphere, *Geophys. Res. Lett., 20,* doi:10.1029/93/GL00212.

Daniel, J. S. and G. J. M Velders (Lead Authors), A. R. Douglass, P. M. D. Forster, D. A. Hauglustaine, I. S. A. Isaksen, L. J. M. Kuijpers, A. McCulloch and T. J. Wallington (2007), Halocarbon scenarios, ozone depletion potentials, and global warming potentials, Chapter 8 in *Scientific Assessment of Ozone Depletion: 2006*, Global Ozone Research and Monitoring Project Report No. 50, World Meteorological Organization, Geneva, Switzerland.

Davies, T., M. J. P. Cullen, A. J. Malcolm, M. H. Mawson, A. Staniforth, A. A. White, and N. Wood (2005), A new dynamical core for the Met Office's global and regional modelling of the atmosphere, *Q. J. R. Meteorol. Soc., 131*, 1759–1782, doi:10.1256/qj.04.101.

Déqué, M. (2007), Frequency of precipitation and temperature extremes over France in an anthropogenic scenario: Model results and statistical correction according to observed values, *Global Planet. Change, 57*, 16–26, doi:10.1016/j.gloplacha.2006.11.030.

de Grandpré, J., S. R. Beagley, V. I. Fomichev, E. Griffioen, J. C.McConnell, A. S. Medvedev, and T. G. Shepherd (2000), Ozone climatology using interactive chemistry: Results from the Canadian Middle Atmosphere Model, *J. Geophys. Res., 105*, 26,475–26,491, doi:10.1029/ 2000JD900427.

Douglass, A. R. and V. Fioletov (Coordinating Lead Authors), S. Godin-Beekman, R. Müller, R. S. Stolarski, and A. Webb (2011), Stratospheric Ozone and Surface

Ultraviolet Radiation, Chapter 2 in *Scientific Assessment of Ozone Depletion: 2010,* Global Ozone Research and Monitoring Project Report No. 52, World Meteorological Organization, Geneva, Switzerland.

Douglass, A. R., R. B. Rood and R. S. Stolarski (1985), Interpretation of ozone temperature correlations: 2. Analysis of SBUV ozone data, *J. Geophys. Res., 90,* 10,693-10,708.

Douglass, A. R. and R. B. Rood (1986), Derivation of photochemical information near 1 mbar from ozone and temperature data, *J. Geophys. Res., 91,* 13,153-13,166.

Froidevaux L., M. Allen, S. Berman, A. Daughton (1989), The mean ozone profile and its temperature sensitivity in the upper stratosphere and lower mesosphere – an analysis of LIMS observations, *J. Geophys. Res., 94,* 6389-6417.

Garcia, R. R., D. Marsh, D. E. Kinnison, B. Boville, and F. Sassi (2007), Simulations of secular trends in the middle atmosphere, 1950–2003, *J. Geophys. Res., 112,* D09301, doi:10.1029/2006JD007485.

Gordley, L. L. et al. (1996), Validation of nitric oxide and nitrogen dioxide measurements made by the halogen occultation experiment for UARS platform, *J. Geophys. Res., 101,* 10241-10266.

Hartmann D. L. and R. R. Garcia (1979), Mechanistic model of ozone transport by planetary waves, *J. Atmos. Sci., 36,* 350-364.

Hood L. L. and A. R. Douglass (1988), Stratospheric responses to solar ultraviolet variations – comparisons with photochemical models, *J. Geophys. Res., 93,* 3905-3911.

IPCC (Intergovernmental Panel on Climate Change) (2000), *Special Report on Emissions Scenarios: A Special Report of Working Group III of the Intergovernmental Panel on Climate Change,* 599 pp., Cambridge Univ. Press, Cambridge, U. K.

Jourdain, L., S. Bekki, F. Lott and F. Lefevre (2008), The coupled chemistry-climate model LMDZ-REPROBUS: Description and evaluation of a transient simulation of the period 1980 – 1999, *Ann. Geophys., 26,* 1391-1413, doi:10.5194/angeo-26-1391-2008.

Johnston, H. S. and J. Podolske (1978), Interpretations of stratospheric photochemistry, *Rev. Geophys., 16,* 491-520.

Lipson, J. B., T. W. Beiderhase, L. T. Molina, M. J. Molina, M. Olzmann (1999), Production of HCl in the OH + ClO reaction: Laboratory measurements and Statistical Rate Theory Calculations, *J. Chem. Phys. A, 103,* 2665-2673.

Livesey J., et al. (2010), Earth Observing System Aura Microwave Limb Sounder ersion 3.3 Level 2 data quality and description document, JPL D-33509, Jet Propulsion Laboratory, Pasadena, CA.*http://mls.jpl.nasa.gov/*.

McCormack, J. P., S. D. Eckermann, D. E. Siskind and T. J. McGee (2006), CHEM2D-OPP: A new linearized gas-phase ozone photochemistry parameterization for high-altitude NEP and climate models, *Atmos. Chem. Phys., 6*, 4943-4972.

Morgenstern, O., P. Braesicke, F. M. O'Connor, A. C. Bushell, C. E. Johnson, S. M. Osprey, and J. A. Pyle (2009), Evaluation of the new UKCA climate composition model. Part 1: The stratosphere, *Geosci. Model Dev., 2*, 43–57, doi:10.5194/gmd-2-43-2009.

Nagatani, R. M. and A. J. Miller (1984), Stratospheric ozone changes during the first year of SBUV Observations. *J. Geophys. Res., 89*, 5191-5198.

Newchurch, M. J., E.-S. Yang, D. M. Cunnold, G. C. Reinsel, J. M. Zawodny, and J. M. Russell III (2003), Evidence for slowdown in stratospheric ozone loss: First stage of ozone recovery, *J. Geophys. Res.*, 108, 4507, doi:10.1029/2003JD003471.

Oman, L. D. et al. (2010), Multimodel assessment of the factors driving stratospheric ozone evolution over the 21$^{st}$ century, *J. Geophys. Res., 115*, D24306, doi:10.1029/2010JD014362, 1011.

Pawson, S., R. S. Stolarski, A. R. Douglass, P. A. Newman, J. E. Nielsen, S. M. Frith, and M. L. Gupta (2008), Goddard Earth Observing System chemistry-climate model simulations of stratospheric ozone-temperature between 1950 and 2005, *J. Geophys. Res., 113*, D12103, doi:101029/2007JD009511.

Pitari, G., E. Mancini, V. Rizi, and D. T. Shindell (2002), Impact of future climate and emission changes on stratospheric aerosols and ozone, *J. Atmos. Sci., 59*, 414–440, doi:10.1175/1520-0469(2002)059<0414: IOFCAE>2.0.CO;2.

Randel, W. J. (1993), Global variations of zonal mean ozone during stratospheric warming events, *J. Atmos. Sci., 50*, 3308 – 3321.

Reber, C. A., C. E. Trevathan, R. J. McNeal, and M. R. Luther (1993), The Upper Atmosphere Research Satellite (UARS) mission, *J. Geophys. Res., 98*, 10,643-10,647.

Rood, R. B., and A. R. Douglass (1985), Interpretation of ozone temperature correlations: 1. Theory, *J. Geophys. Res., 90*, 5733-5743.

Rosenfield, J. E. and A. R. Douglass (1998), Doubled $CO_2$ effects on $NO_Y$ in a Coupled 2D Model, *Geophys. Res. Lett., 90*, 4381-4384.

Russell, J. M., et al. (1993), The Halogen Occultation Experiment, *J. Geophys. Res., 98,* 10777-10797.

Sander, S. P., J. Abbatt, J. R. Barker, J. B. Burkholder, R. R. Friedl, D. M. Golden, R. E. Huie, C. E. Kolb, M. J. Kurylo, G. K. Moortgat, V. L. Orkin and P. H. Wine (2011), Chemical Kinetics and Photochemical Data for Use in Atmospheric Studies, Evaluation No. 17, JPL Publication 10-6, Jet Propulsion Laboratory, Pasadena, http://jpldataeval.jpl.nasa.gov.

Schraner, M., et al. (2008), Technical Note: Chemistry-climate model SOCOL: Version 2.0 with improved transport and chemistry/microphysics schemes, *Atmos. Chem. Phys., 8,* 5957–5974, doi:10.5194/acp-8-5957-2008.

Scinocca, J. F., N. A. McFarlane, M. Lazare, J. Li, and D. Plummer (2008), Technical note: The CCCma third generation AGCM and its extension into the middle atmosphere, *Atmos. Chem. Phys., 8,* 7055–7074, doi:10.5194/acp-8-7055-2008.

Shibata, K., and M. Deushi (2008a), Long-term variations and trends in the simulation of the middle atmosphere 1980–2004 by the chemistry climate model of the Meteorological Research Institute, *Ann. Geophys., 26,* 1299–1326, doi:10.5194/angeo-26-1299-2008.

Shibata, K., and M. Deushi (2008b), Simulation of the stratospheric circulation and ozone during the recent past (1980 – 2004) with the MRI chemistry-climate model, CGER's Supercomp. Monogr. Rep., 14, 154pp., Cent for Gobal Environ. Res., Natl. Inst. For Environ. Studies, Tsukuba, Japan.

Smith, A. K. (1995), Numerical simulation of global variations of temperature, ozone and trace species in the stratosphere, *J. Geophys. Res., 100,* 1253-1269.

SPARC CCMVal, SPARC CCMVal Report on the Evaluation of Chemistry-Climate Models (2010), V. Eyring, T. G. Shepherd, D. W. Waugh (Eds.), SPARC Report No. 5, WCRP-132, WMO/TD-No. 1526, http://www.atmosp.physics.utoronto.ca/SPARC.

Stolarski, R. S., and A. R. Douglass (1985), Parameterization of the photochemistry of stratospheric ozone including catalytic loss processes, *J. Geophys. Res., 90,* 10,709-10,718.

Stolarski, R. S., A. R. Douglass, P. A. Newman, S. Pawson, M. R. Schoeberl (2010), Relative contribution of greenhouse gases and ozone-depleting substances to temperature trends in the stratosphere: A chemistry-climate model study, *J. Clim., 23,* 28-42.

Stolarski R. S., A. R. Douglass, E. E. Remsberg, N. J. Livesey, J. C. Gille (2011), Ozone temperature correlations in the upper stratosphere as a measure of chlorine content, *submitted to JGR.*

Strahan, S. et al. (2011), Using transport diagnostics to understand chemistry climate model ozone simulations, *J. Geophys. Res., 116,* D17302, doi:10.1029/2010D015360.

Teyssèdre, H., et al. (2007), A new tropospheric and stratospheric chemistry and transport model MOCAGE-Climat for multi-year studies: Evaluation of the present-day climatology and sensitivity to surface processes, *Atmos. Chem. Phys., 7,* 5815–5860, doi:10.5194/acp-7-5815-2007.

Tian, W., and M. P. Chipperfield (2005), A new coupled chemistry-climate of the stratosphere: The importance of coupling for future O3-climate predictions, *Q. J. R. Meteorol. Soc., 131,* 281-303, doi:10.1256/qj.04.05.

Tian, W., M. P. Chipperfield, L. J. Gray, and J. M. Zawodny (2006), Quasibiennial oscillation and tracer distributions in a coupled chemistry-climate model, *J. Geophys. Res., 111,* D20301, doi:10.1029/2005JD006871.

Wang, P.-H., M. P. McCormick and W. P. Chu (1983), A study on the planetary wave transport of ozone during the late February 1979 stratospheric warming using the SAGE ozone observation and meteorological information, *J. Atmos. Sci., 40,* 2419-2431.

Water, J. W., et al. (2006), The Earth Observing System Microwave Limb Sounter (EOS MLS) on the Aura Satellite, *IEEE Trans. Geosci. Remote Sens. 44,* 1075-1092.

Waugh, D. W. and V. Eyring (2008), Quantitative performance metrics for stratospheric-resolving chemistry-climate models, *Atmos. Chem. Phys., 8,* 5699-5713.

WMO (World Meteorological Organization) (2007), *Scientific Assessment of Ozone Depletion: 2006,* Global Ozone Research and Monitoring Project, Rep. 50, 572 pp., Geneva, Switzerland.

WMO (World Meteorological Organization) (2011), *Scientific Assessment of Ozone Depletion: 2010:* Global Ozone Research and Monitoring Project – Report No. 52, 516 pp., Geneva, Switzerland.

Table 1 – CCMVal models with a vertical domain including the upper stratosphere and also submitted future simulations for the 2010 CCMVal report and for WMO 2011.

| Model | Reference |
|---|---|
| AMTRAC3 | *Austin and Wilson* [2010] |
| CCSRNIES | *Akiyoshi et al.* [2009] |
| CMAM | *Scinocca et al.* [2008]; *de Granspré et al.* [2010] |
| CNRM-ACM | Déqué [2007]; *Teyssièdre et al.* [2007] |
| GEOSCCM | *Pawson et al.* [2008] |
| LMDZrepro | *Jourdain et al.* [2008] |
| MRI | *Shibata and Deushi [2008a; 2008b]* |
| Niwa-SOCOL | *Schraner et al.* [2008] |
| SOCOL | *Schraner et al.* [2008] |
| ULAQ | *Pitari et al.* [2002] |
| UMSLIMCAT | *Tian and Chipperfield* [2005]; *Tian et al.* [2006] |
| UMUKCA-METO | *Davies et al.* [2005]; *Morgenstern et al.* [2009] |
| UMUKCA-UCAM | *Davies et al.* [2005]; *Morgenstern et al.* [2009] |
| WACCM | *Garcia et al.* [2007] |

Table 2

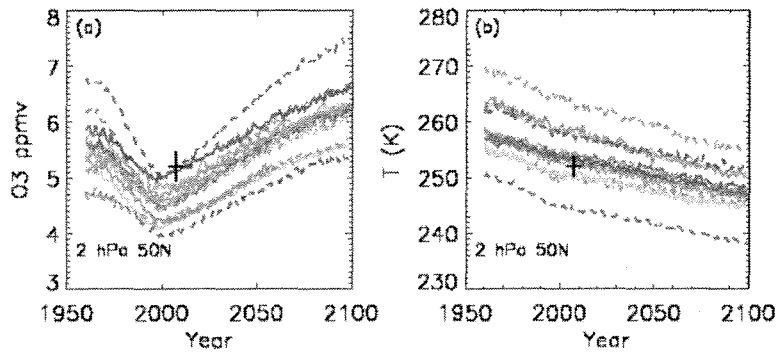| Chemical Family | Rate Limiting Reactions |
|---|---|
| Oxygen | $O + O_3$ |
| Nitrogen | $O + NO_2$ |
| Hydrogen | $O + OH; O + HO_2; O_3 + HO_2; H + O_2 + M$ |
| Chlorine | $O + ClO$ |

Figure 1:  Time series for annual zonal mean ozone mixing ratio (left) and temperature (right) at 50°N 2 hPa from the CCMVal models listed in Table 1.
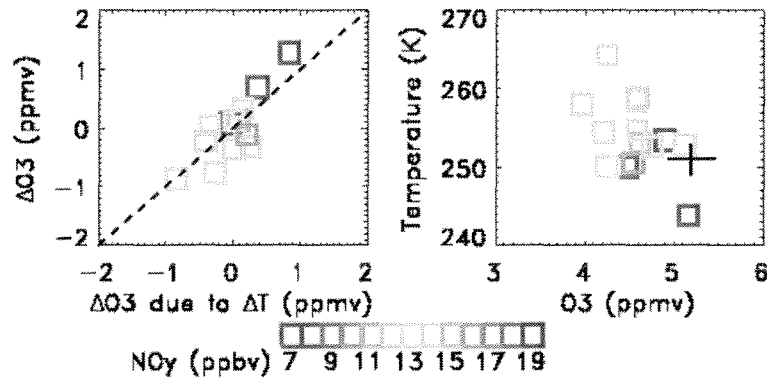


Figure 2:   (a) The 1960 50°N 2 hPa ozone difference from the multimodel mean ($\gamma_{O3}$ - $\gamma_{O3}^{MM}$, y-axis) is approximated for each model by its sensitivity of ozone to temperature times the temperature difference from the multimodel mean ($\partial\gamma_{O3}/\partial T *(T - T^{MM})$, x-axis). In both panels points for each model are colored according to the annually averaged local $NO_Y$ mixing ratio.   (b) Simulated values for 2006 annual mean temperature and ozone at the same location also show the association of cooler temperature with higher ozone and vice versa.  The large cross indicates annual mean ozone and temperature calculated from MLS observations for 2005-2010; the size of the cross indicates estimated accuracies.
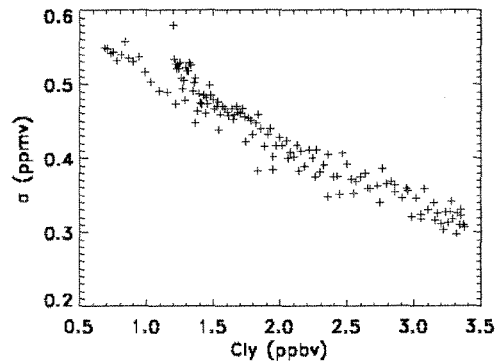
22

Figure 3: The standard deviation of annual mean ozone at 50°N 2 hPa as computed from the CCMVal simulations varies nearly linearly with upper stratospheric chlorine level, and is minimal when the chlorine level is highest.
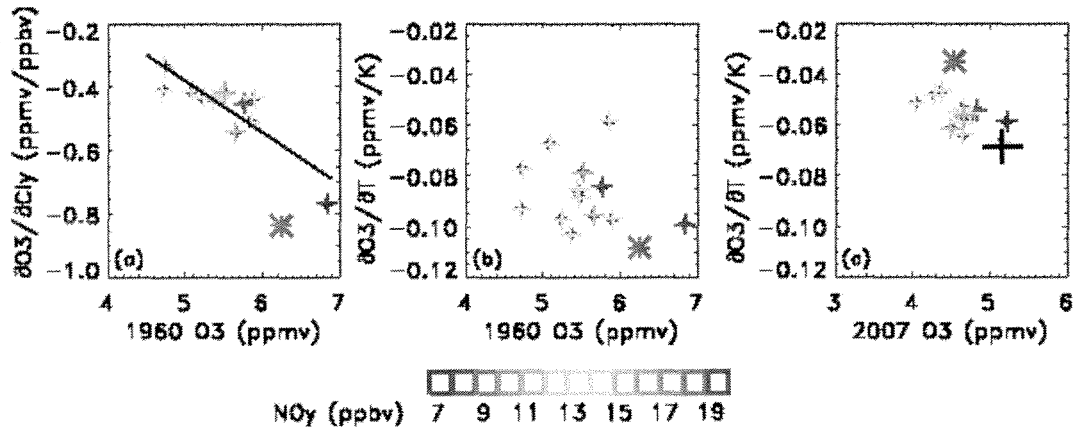


Figure 4: (a) Sensitivity of ozone to chlorine change at 50°N 2hPa obtained from MLR as a function of 1960 ozone mixing ratio. Colors indicate $NO_Y$ levels. Star is the MRI model that is more sensitive to chlorine because of a missing reaction. Solid line is a linear fit excluding the MRI model. (b) Sensitivity of ozone to temperature obtained from the MLR as a function of 1960 ozone mixing ratio. Simulations with higher initial ozone are generally more sensitive to temperature than those with lower ozone levels. (c) Sensitivity of ozone to temperature obtained from 2007 seasonal cycle as a function of the 2007 ozone mixing ratio. The large cross shows values obtained from MLS observations assuming 5 percent error in the ozone mixing ratio and 10% error in the ozone sensitivity to temperature. See text for discussion.
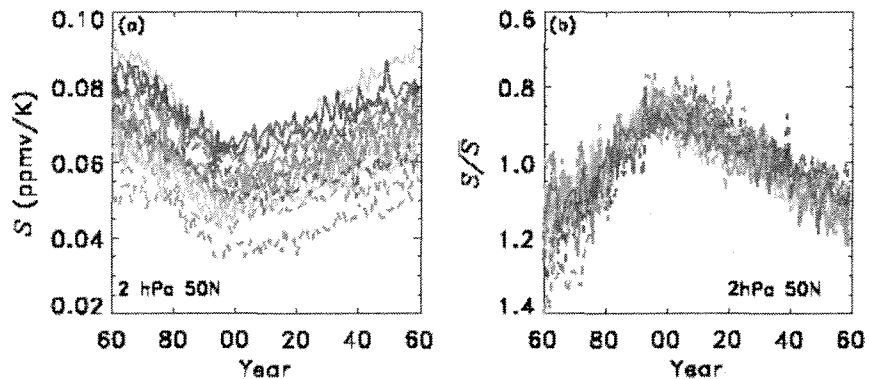
Figure 5: a) Time series for $S$ (sensitivity of ozone to temperature) at 2hPa 50°N as determined for each model from the annual cycles in ozone and temperature; b) Same time series for $S$ as in (a) but divided by the 100-year mean for each simulation.
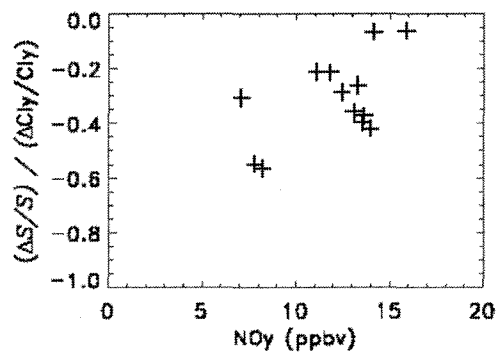


Figure 6: The logarithmic derivative of S divided by the logarithmic derivative of the chlorine mixing ratio as a function of local 1960 $NO_Y$ mixing ratio at 50°N 2 hPa (crosses).